Parity anomaly driven topological transitions in magnetic field

J. Böttcher and E. M. Hankiewicz*
Institut für Theoretische Physik und Astronomie, Universität Würzburg, 97074 Würzburg, Germany

(Dated: July 28, 2016)

Recent developments in solid state physics give a prospect to observe the parity anomaly in (2+1)D massive Dirac systems. Here we show, that the quantum anomalous Hall (QAH) state in orbital magnetic fields originates from the Dirac mass term and induces an anomalous four-current related to the parity anomaly. This differentiates the QAH from the quantum Hall (QH) state for the experimentally relevant case of an effective constant density (seen by the gate). A direct signature of QAH phase in magnetic fields is a long $\sigma_{xy} = e^2/h$ ($\sigma_{xy} = -e^2/h$) plateau in $Cr_x(Bi_{1-y}Sb_y)_{2-x}Te_3$ (HgMnTe quantum wells). Furthermore, we predict a new transition between the quantum spin Hall (QSH) and the QAH state in magnetic fields, for constant effective carrier density, without magnetic impurities but driven by effective g-factors and particle-hole asymmetry. This transition can be related to the stability of edge states in the Dirac mass gap of 2D topological insulators (TIs), even in high magnetic fields.

Introduction: Condensed matter analogs of the (2+1)D and (3+1)D Dirac equation, i.e. topological insulators (TI) and Weyl semimetals, opened new directions to study high energy anomalies in the solid state lab. An anomaly in high energy physics is defined as breaking of a classical symmetry during regularization [1] and, in particular, the parity anomaly is characterized by a broken parity symmetry in a quantized theory. For instance in case of the massless Dirac equation in (2+1)D, coupled to an electromagnetic field, parity symmetry is violated if one insists on gauge-invariance [2–7]. In solid state physics on the other hand, "parity anomaly" is often understood as generation of an anomalous four-current related to a finite mass term in the Dirac equation [8, 9]. Anytime when we relate to the notion of "parity anomaly", we refer to the second definition.

At first glance, chiral currents related to the massive Dirac equation in (2+1)D, coupled to an electromagnetic field, appear similar to chiral currents associated with the QH effect (quantization of Hall conductance in a two-dimensional (2D) electron gas in an external out-of-plane magnetic field [10, 11]). However, in case of the "parity anomaly" the current is induced by the mass term (violating parity), while the current in the QH phase is induced by magnetic field (no violation of parity) [5, 12]. Despite a plethora of suggestions for possible realizations of the "parity anomaly" in a condensed matter system, its experimental observation is still outstanding [13–15].

Recently new topological states of matter have been discovered such as 2D TIs characterized by the QSH effect where an odd number of pairs of counterpropagating (helical) edge states exist at the boundary [16–20]. When 2D TIs [21, 22] or thin films of 3D TIs [23–25] are doped with magnetic impurities, the gap for one of the spin directions can be closed due to broken time-reversal symmetry (TRS) and QAH effect forms. It is characterized by a single propagating chiral edge state existing even in the absence of magnetic field. When both TRS and particle-hole symmetry (PHS) are broken QSH, QAH and QH phases are all classified by a Z-topological invariant [26, 27]. Outstanding questions then arise, whether any of these effects are related to the "parity anomaly" and if their experimental distinction is possible in an external magnetic field. Answering these questions is the goal of this paper.

The QSH phase is described by two copies of massive (2+1)D Dirac Hamiltonians [18]. As we will show in this paper, there is an anomalous four-current for each single block, indexed by $i = \{1, 2\}$, if the chemical potential lies in the mass gap:

$$j_\mu^{(i)} = (-1)^{i+1} \frac{e^2}{4h} \left[\mathrm{sgn}(M) + \mathrm{sgn}(B)\right] \epsilon_{\mu\nu\tau} F^{\nu\tau}, \qquad (1)$$

where $F_{\nu\tau} = \partial_\nu A_\tau - \partial_\tau A_\nu$ is the electromagnetic tensor, while M and B are the relativistic Dirac mass and the effective mass originating from quadratic dispersion (Newtonian mass) [9], respectively.

Sum and difference of anomalous four-currents, $j_\mu^\pm = j_\mu^{(1)} \pm j_\mu^{(2)}$, can be used to distinguish between QH, QAH and QSH phases in magnetic field. Although the helical edge states of the QSH phase are not anymore protected against backscattering in magnetic fields (due to broken TRS [9, 28]) as long as neither M nor B change their sign as a function of the magnetic field, j_μ^- remains nonzero. We denote this phase QSH-like (QSHL) phase. Similarly, the QAH state is characterized by a nonzero j_μ^+ as well as j_μ^- in magnetic field and we denote this phase QAH-like (QAHL) [29]. Chiral edge states related to the QAHL phase form in the mass gap and are therefore distinct from QH edge states which form above the mass gap and have Hall currents scaling as the sign of magnetic field [12].

As pointed out by Ma et al. [30], the effective carrier density and not the chemical potential can be accessed by

a gate electrode in a typical experimental set-up. However, topological transitions in magnetic field have been so far mostly analyzed in terms of constant chemical potential [19]. Therefore, we predict in this paper new types of topological transitions in magnetic field at constant effective carrier density. Under this condition, we show that the "parity anomaly" allows for a unique distinction of the QAHL and QH phases in magnetic fields. In particular, we predict a long Hall plateau at $\sigma_{xy} = -e^2/h$ ($\sigma_{xy} = e^2/h$), related to the QAHL phase of HgMnTe ($Cr_x\left(Bi_{1-y}Sb_y\right)_{2-x}Te_3$) [24, 25]. Moreover, we predict a new topological QSH to QAHL transition, occurring without any magnetization but as a consequence of the particle-hole asymmetry and effective g-factors. This latter transition might be related to the recent observation of stable edge states of 2D TIs in the mass gap for high magnetic fields [30, 31].

Model: Let us consider the BHZ Hamiltonian, i.e. a two flavor-(2+1)D massive Dirac Hamiltonian [32], describing 2D TIs, [18]

$$\mathcal{H}(\mathbf{k}) = \begin{pmatrix} h_+(\mathbf{k}) & 0 \\ 0 & h_-(\mathbf{k}) \end{pmatrix} + \mathcal{H}_z(H_0) + \mathcal{H}_{ex}, \quad (2)$$

$$h_\pm(\mathbf{k}) = \epsilon(\mathbf{k})\sigma_0 \pm M(\mathbf{k})\sigma_3 \pm A(k_x\sigma_1 + k_y\sigma_2), \quad (3)$$

$$\mathcal{H}_z(H_0) = \mathrm{Diag}\left(-g_E \;\; -g_H \;\; g_H \;\; g_E\right) H_0, \quad (4)$$

$$\mathcal{H}_{ex} = \mathrm{Diag}\left(-\chi_E \;\; -\chi_H \;\; \chi_H \;\; \chi_E\right), \quad (5)$$

written in the Dirac basis, i.e. in the low energy subbands $\{|E1,\downarrow\rangle, -|H1,\downarrow\rangle, -|H1,\uparrow\rangle, |E1,\uparrow\rangle\}$. Here, $\epsilon(\mathbf{k}) = -Dk^2$, $M(\mathbf{k}) = M - Bk^2$, $\mathbf{k}^\intercal = \begin{pmatrix} k_x & k_y \end{pmatrix}$, $k^2 = k_x^2 + k_y^2$, $k_\pm = k_x \pm ik_y$ and D, M, B and A are system parameters. $\mathcal{H}_z$ denotes a Zeeman Hamiltonian and $\mathcal{H}_{ex}$ describes exchange interaction between s/p-band electrons with localized spins belonging to the magnetic impurities. For HgMnTe [33], the exchange coupling is paramagnetic [21], while it is ferromagnetic for $Cr_x\left(Bi_{1-y}Sb_y\right)_{2-x}Te_3$ [23]. In the following, we demand that the chemical potential is placed in the Dirac mass gap at zero magnetic field such that the system is insulating in the bulk.

Let us first study the bulk Landau level (LL) spectrum of the spin-up block. We consider an external magnetic field $\boldsymbol{H}$ oriented perpendicular to the plane of the 2D electron gas, $\boldsymbol{H} = H_0\mathbf{e}_z$, with $H_0 > 0$. The orbital effect of the magnetic field is introduced by the Peierls substitution $\mathbf{k} \to \mathbf{k} + e/\hbar\mathbf{A}$ ($e > 0$), using the Landau gauge $\mathbf{A} = -yH_0\mathbf{e}_x$. The bulk LL spectrum is obtained using ladder operators $k_- = \sqrt{2}/l_H\hat{a}$ and $k_+ = \sqrt{2}/l_H\hat{a}^\dagger$ fulfilling the usual commutation relation $\left[\hat{a}, \hat{a}^\dagger\right] = 1$, where $l_H = \sqrt{\hbar/eH_0}$ is the magnetic length. This can be used to construct an ansatz for the Schrödinger equation [19],

$$\psi_\uparrow^{k_x,n\neq 0} = \left(u_1|n-1\rangle \;\; u_2|n\rangle\right)^\intercal, \quad (6)$$

$$\psi_\uparrow^{k_x,n=0} = \left(\begin{array}{cc} 0 & |0\rangle \end{array}\right)^\intercal, \quad (7)$$

where n is the LL index and k_x is a good quantum number. The resulting spectrum is given by

$$E^\pm_{\uparrow,n>0} = \frac{g_1-\beta}{2} - n\delta \pm \sqrt{n\alpha^2 + \left(M^\star_\uparrow(H_0) - n\beta\right)^2} \quad (8)$$

$$E_{\uparrow,n=0} = M + \frac{g_1+g_2-\beta-\delta}{2}, \quad (9)$$

where $\alpha = \sqrt{2}A/l_H$, $\beta = 2B/l_H^2$ and $\delta = 2D/l_H^2$, $g_{1/2} = (\chi_E + g_E H_0) \pm (\chi_H + g_H H_0)$ and

$$M^\star_\uparrow(H_0) = M + g^\star(H_0), \quad (10)$$

where $g^\star(H_0) = \left(g_2(H_0) - \delta(H_0)\right)/2$ is the effective g-factor. Since $M^\star_\uparrow(H_0)$ transforms under parity as the usual Dirac mass M, it can be interpreted as the renormalized Dirac mass in an external magnetic field and it replaces M in Eq. (1). More details on the symmetry of the BHZ Hamiltonian are given in Appendix B. It is apparent that even for $\chi_E = \chi_H = g_E = g_H = 0$ the effective g-factor is nonzero due to a broken PHS.

For $n \neq 0$, all LLs come in particle/hole pairs reproducing the bulk band gap in the limit $H_0 \to 0$. However, the $n = 0$ LL lacks a partner [15] and its respective chiral edge state goes through the mass gap in case of the topologically non-trivial regime $M^\star_\uparrow(0)/B > 0$.

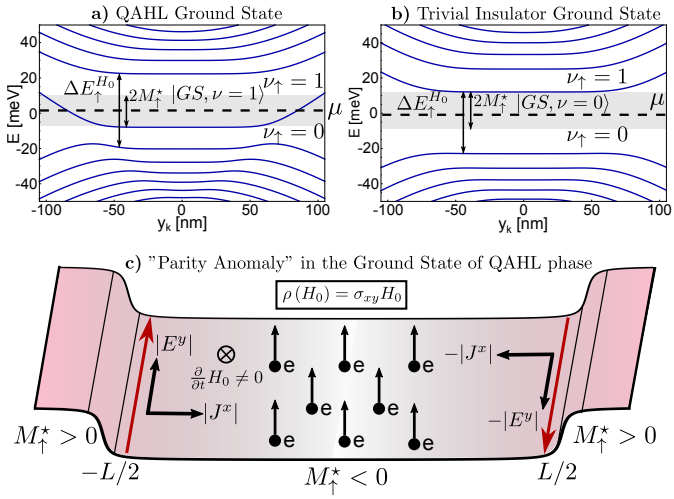

FIG. 1. Spectrum of spin-up block of BHZ Hamiltonian for **(a)** QAHL $\nu = 1$ and **(b)** a trivial insulator $\nu = 0$ in magnetic fields. $\nu_\downarrow = 0$ state is not shown and stays constant across the transition. The magnetic gap is given by $\Delta E^{H_0}_\uparrow$ and the mass gap by $M^\star_\uparrow$. For the trivial insulator, both the bare charge ρ and the effective charge $\rho^\star$ are equal to zero (see main text). **(c)** Schematic view of charge pumping in ground state of QAHL insulator. For QAHL system an adiabatic increase of the magnetic field H_0 causes a circulating electric field. At the mass domain wall, indicated by the colored landscape, chiral edge states form and charges flow from the domain wall to the bulk as a response to the electric field. Due to the "parity anomaly", an additional topological term occurs in the Chern-Simons action of a QAHL system such that the net charge/electric field is zero, $\rho^* = 0$ but $\rho \neq 0$. Black arrows represent schematically flux quanta attached to the electrons.

Trivial versus QAHL phases in orbital magnetic fields: Here, we study the difference between trivial insulating and QAHL phases in magnetic fields. The QAHL phase is characterized by $\nu = \nu_\uparrow + \nu_\downarrow = 1$, while the trivial insulator has $\nu = 0$. Since the two blocks in Eq. (2) are decoupled, we focus on the spin-up block $h_-(\mathbf{k})$ ($\nu_\uparrow = 1$) and omit the trivial ($\nu_\downarrow = 0$) spin-down block. Details of the calculation are given in Appendix A.

We start the discussion from the QAH state with $\nu = 1$, where the ground state is defined by $|vac\rangle = \prod_{k_x,k_y} a^\dagger_{-,\uparrow}(k_x,k_y)|0\rangle$ and the minus sign denotes that only valence band states are filled. Adiabatically switching on the magnetic field induces an azimuthal electric field, since $\nabla \times \mathbf{E} = -\partial/\partial t\, H_0$. Based on a semi-classical calculation [34–36], it is easy to show that an anomalous four-current is induced,

$$j_\mu = -\frac{e^2}{4h}\left[\mathrm{sgn}\left(M^\star_\uparrow(x)\right) + \mathrm{sgn}\,(B)\right]\epsilon_{\mu\nu\tau}F^{\nu\tau}. \qquad (11)$$

This means that the electric field pump current j_x from the left (right) side of the sample into the bulk, $e^2|E_y|/h$ ($-e^2|E_y|/h$), resulting in a carrier density of $\rho = -e^2H_0/h = -eH_0/\phi_0$ with $\phi_0 = h/e$. This corresponds to filling of the $n = 0$ LL and signs of currents and charges are determined by the sign of the mass, $M^\star_\uparrow$ as schematically indicated in Fig. 1c. Since during the process of switching of H_0, the topological Dirac mass does not close, the question arises: Why does the ground state of QAHL phase change from $\rho = 0$ in a zero magnetic field to a finite value for a non-zero H_0? Does this not break the adiabatic assumption for switching on magnetic field as well as the constraint of constant carrier density in experiments [25, 30, 37]? The solution comes from the fact that QAH and QAHL phases break parity symmetry due to the topological mass, $M^\star_\uparrow(H_0)$ (see Appendix B), which enforces adding a topological Chern-Simons term in the gauge field Lagrangian,

$$\Delta\mathcal{L}_C = \frac{\kappa}{2}\epsilon^{\mu\nu\tau}F_{\mu\nu}A_\tau, \qquad (12)$$

where $\kappa = -e^2\left[\mathrm{sgn}(M^\star_\uparrow(x)) + \mathrm{sgn}(B)\right]/h$ is the Chern-Simons coupling constant, which modifies the Maxwell equation,

$$\nabla\cdot\mathbf{E} = \rho(H_0) + \kappa H_0 \equiv \rho^\star. \qquad (13)$$

The term originating from the Chern-Simons action generates a flux κH_0 which compensates charge such that the full effective charge $\rho^\star$ remains zero ($\rho \neq 0$). When the chemical potential is located within the mass gap at $H_0 = 0$ with $\nu = 1$, it remains in the mass gap for non-zero H_0. Using a half-space calculation, we additionally prove in Appendix D that the $n = 0$ LL makes a transition from the trivial to QAHL insulator at $M^\star_\uparrow(H_0) = 0$ [38, 39]. Even so the discussion was given for a QAHL state with $\nu = 1$, it applies as well for $\nu = -1$. In comparison, a trivial insulator does not break parity symmetry and therefore no intrinsic Chern-Simons term is allowed in the gauge field Lagrangian [12]. This is shown in Fig. 1b, where $\rho = \rho^\star = 0$. This means that QAHL phase has a non-zero Chern number but $\rho^* = 0$ and therefore it has to be counted differently from QH LLs forming above the magnetic gap. Therefore, the "parity anomaly" distinguishes unambiguously QAHL effect from a trivial insulator in magnetic fields.

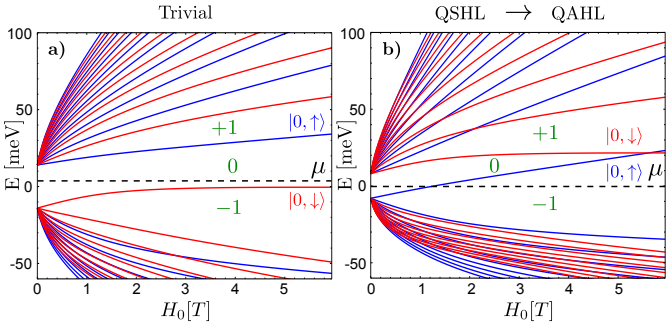

FIG. 2. Landau level fan for **(a)** trivial insulator **(b)** non-trivial 2D TI, where blue and red symbolize spin-up and spin-down LLs, respectively. Both plots are calculated within BHZ model for $Hg_{0.98}Mn_{0.02}Te$ QWs with **(a)** $d = 7$ nm, $M = 14$ meV, $B = -612$ meVnm^2, $D = -440$ meVnm^2, A $= 395$ meVnm, $g_E = 18.6\ \mu_B$, $g_H = -1.2\ \mu_B$ and with **(b)** $d = 10$ nm, $M = -8$ meV, $B = -1070$ meVnm^2, $D = -895$ meVnm^2, A $= 366$ meVnm, $g_E = 29.5\ \mu_B$, $g_H = -1.2\ \mu_B$. $M/B < 0$ ($M/B > 0$) indicates a topologically trivial (non-trivial) phase [9]. At $H_0 = 0$, Mn impurity spins are randomly oriented and the system is in the QSH phase, $\nu = 0$. In a magnetic field, the gap for the spin-up block closes at $H^{crit}_\uparrow = 1.2$ T with a transition to a stable $\sigma_{xy} = -e^2/h$ QAHL plateau. The transition is indicated by crossing of the chemical potential μ with the spin-up $n = 0$ LL. Numbers within plot indicate Chern numbers.

Stable QAHL plateau for $\nu = \pm 1$: Let us now come back to the full BHZ Hamiltonian and compare LL fans for topological trivial and non-trivial insulators. The discussion is given for realistic parameters for HgMnTe [21, 33, 40]. Technical details concerning these parameters are given in Appendix C. $Hg_{0.98}Mn_{0.02}Te$ with $d = 7$ nm is a topologically trivial insulator ($\nu = \nu_\uparrow = \nu_\downarrow = 0$), the chemical potential for an effective charge $\rho = \rho^\star = 0$ lies in the mass gap (Fig. 2 a)) and it remains to be a trivial insulator even for large magnetic fields.

$Hg_{0.98}Mn_{0.02}Te$ with $d = 10$ nm (Fig. 2b) forms QSH phase with $\nu_\uparrow = -\nu_\downarrow = 1$ and $\rho = \rho^* = 0$. For finite H_0, Mn becomes polarized and the mass gap for the spin-up block closes at $M^\star_\uparrow(H^{crit}_\uparrow) = 0$ signalizing formation of a massless Dirac fermion. For $H_0 > H^{crit}$, it is easy to prove (Appendix A) that $\rho = eH_0/\phi_0$ while $\rho^\star = 0$. Across this transition, the system goes into a QAHL $\nu = -1$ phase.

In the literature, topological transitions are often discussed based on the assumption of a constant chemical

potential and the QSH to QAH transition occurs at zero orbital field [19, 22]. Our transition differs from the above mentioned in two aspects: 1) we assume a constant effective density 2) the topological transition happens in finite magnetic fields. Therefore, we claim that even at non-zero magnetic field, one can define QAHL phase with $j_\mu^{(\pm)}$ different from zero. In conclusion, we predict a stable $\nu = -1$ plateau with a Hall conductance $\sigma_{xy} = -e^2/h$ (see Fig. 3) for HgMnTe above critical QW thickness. This prediction is exactly along the lines of recent experiments on HgMnTe [37], where one needs non-zero magnetic field to polarize Mn and observes a stable $\nu = -1$ plateau. Similarly, recent experiments on $Cr_x\,(Bi_{1-y}Sb_y)_{2-x}\,Te_3$ show a stable $\nu = 1$ plateau up to 15T [24, 25]. We believe that indeed these stable plateaus are direct signatures of the "parity anomaly" in these systems and the sign of g-factors determines if the stable plateau occurs for $\nu = 1$ or $\nu = -1$. Furthermore, after crossing of the two $n = 0$ LLs at H^{cross} [38], the adiabatic condition is possibly not anymore valid. We leave the discussion of this point to another paper, assuming for the moment being that the transition to the trivial phase occurs [19].

The experimental signature in case of HgMnTe is therefore reentrant behavior of the Hall conductance starting from $\sigma_{xy} = 0$ in the QSH phase, changing to $\sigma_{xy} = -1$ in the QAHL state, and reentering $\sigma_{xy} = 0$ plateau for $H_0 > H^{cross}$ (see Fig. 3).

We have omitted off-diagonal terms connecting the two Dirac Hamiltonians such as Rashba spin-orbit interaction terms [41, 42] or bulk-inversion asymmetry terms [19]. They should be small in comparison to diagonal terms and should only renormalize the effective mass gap slightly [43]. Topological transitions in magnetic fields are induced by mass gaps closing and as long as these off-diagonal terms do not close the gap, we expect that only the critical magnetic field might deviate from our prediction. (see also Appendix B).

QSHL to QAHL transition in non-magnetic TIs: Another hallmark of the "parity anomaly" is a transition from a QSHL into a QAHL phase in magnetic fields even without magnetic impurities. As pointed out before, for HgMnTe QWs the exchange interaction is paramagnetic and, therefore, magnetic field dependent [22]. Values of the critical field $H_\uparrow^{crit}$ must be therefore found numerically. However, if we omit exchange coupling ($\chi_E = \chi_H = 0$), one obtains an analytical expression for a transition from the QSH phase to QAHL phase. Closing of the gap for a spin-up block corresponds to $M_\uparrow^\star(H_\uparrow^{crit}) = 0$ with $H_\uparrow^{crit} = -M_\uparrow^\star(0)/g^\star$, where $g^\star = (g_E - g_H)/2 - 2\pi D/\phi_0$ is the effective g-factor without exchange interaction. Interestingly this transition can occur without any magnetization or magnetic impurities but purely from the particle-hole asymmetry and effective g-factors terms which act in magnetic field as the mass connected with the "parity anomaly". We expect that in the QAHL phase, the Hall conductance of the edge states should be more precisely quantized in comparison to the QSHL phase and survive even in large magnetic fields (due to lack of backscattering). In particular, we predict a transition from QSHL phase, characterized by a local two-terminal conductance of $2e^2/h$, to a QAHL phase at $H_{crit}^\uparrow$, characterized by $\sigma_{xx} = e^2/h$, and finally to the trivial phase at H^{cross} (see green dashed line in Fig. 3). Therefore, our prediction of surviving topological edge states in high magnetic fields could be related to the recent observation in Ref. [30].

Summarizing, we have studied topological transitions in magnetic fields for a two-flavour (2+1)D massive Dirac Hamiltonian. We have studied the experimentally relevant case of an effective constant carrier density with the chemical potential located within the mass gap. We have demonstrated that the QAHL phase (QAH effect in orbital magnetic fields) can be distinguished from the QH phase since the former one is a direct consequence of the "parity anomaly" for massive Dirac systems. We have shown that a long $\nu = -1$ and $\nu = 1$ plateaus in HgMnTe and $Cr_x\,(Bi_{1-y}Sb_y)_{2-x}\,Te_3$, respectively, are direct signatures of QAHL phase. Moreover Appendix A, we have predicted a new topological transition from the QSH phase to the QAHL phase without magnetization or magnetic impurities, which can explain the stability of edge states in recent experiments [30].

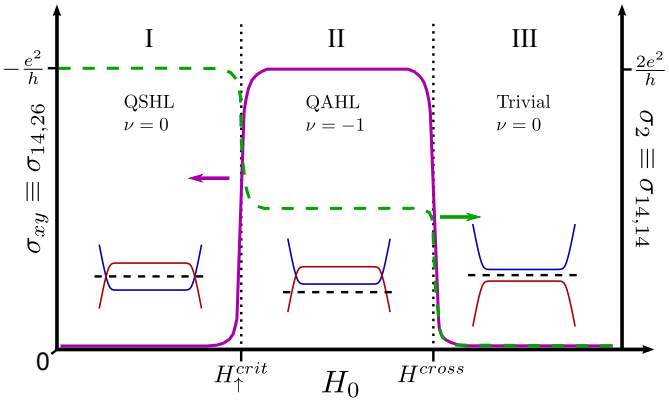

FIG. 3. Transition from the QSHL to the QAHL and finally to the trivial insulator as a function of the magnetic field H_0. Left axis corresponds to the non-local four-terminal Hall conductance, σ_{xy} (as for example in [37]), while the right axis to the local two-terminal longitudinal conductance, σ_{xx} (as for example in [30]). To highlight transitions we subdivided the plot in three areas. In the insets the blue and red lines show schematically the $n = 0$ LLs and the black dashed line shows the position of the chemical potential in the ground state. $\sigma_{xy} = 0$ for $H_0 < H_\uparrow^{crit}$ for QSHL effect. The transition to QAHL phase with a $\sigma_{xy} = -e^2/h$ occurs at $H_\uparrow^{crit}$ by virtue of the "parity anomaly". At the crossing point of the two $n = 0$ LL, H^{cross}, the system might become trivial (see main text). The $\sigma_{xx} = 2e^2/h$ in the QSHL phase changes to e^2/h at $H_\uparrow^{crit}$ (QAHL phase), and possibly to zero at H^{cross}.

Acknowledgments. We thank F. Wilczek, B. A. Bernevig, C. Brüne, L. W. Molenkamp, C. Kleiner, J. S. Hofmann, J. Erdmenger, C. Morais Smith and W. Beugeling for useful discussions. We acknowledge financial support from the DFG via SFB 1170 "ToCoTronics", and the ENB Graduate School on Topological Insulators.

* hankiewicz@physik.uni-wuerzburg.de

[1] R. A. Bertlmann, *Anomalies in Quantum Field Theory*, edited by R. A. Bertlmann (Oxford University Press, 1996).
[2] S. Deser, R. Jackiw, and S. Templeton, Annals of Physics **140**, 372 (1982).
[3] R. Jackiw, Phys. Rev. D **29**, 2375 (1984).
[4] A. N. Redlich, Phys. Rev. Lett. **52**, 18 (1984).
[5] D. Boyanovsky, R. Blankenbecler, and R. Yahalom, Nuc. Phys. **B270**, 483 (1986).
[6] H. B. Nielsen and M. Ninomiya, Nuc. Phys. B **185**, 20 (1981).
[7] H. B. Nielsen and M. Ninomiya, Nuc. Phys. B **193**, 173 (1981).
[8] M. Stone and F. Gaitan, Annals of Physics **178**, 89 (1987).
[9] X.-L. Qi and S.-C. Zhang, Rev. Mod. Phys. **83**, 1057 (2011).
[10] D. J. Thouless, M. Kohmoto, M. P. Nightingale, and M. den Nijs, Phys. Rev. Lett. **49**, 405 (1982).
[11] Y. Hatsugai, Phys. Rev. Lett. **71**, 3697 (1993).
[12] A. Abouelsaood, Phys. Rev. Lett. **54**, 1973 (1985).
[13] G. W. Semenoff, Phys. Rev. Lett. **53**, 2449 (1984).
[14] E. Fradkin, E. Dagotto, and D. Boyanovsky, Phys. Rev. Lett. **57**, 2967 (1986).
[15] F. D. M. Haldane, Phys. Rev. Lett. **61**, 2015 (1988).
[16] C. L. Kane and E. J. Mele, Phys. Rev. Lett. **95**, 226801 (2005).
[17] C. L. Kane and E. J. Mele, Phys. Rev. Lett. **95**, 146802 (2005).
[18] B. A. Bernevig, T. L. Hughes, and S.-C. Zhang, Science **314**, 1757 (2006).
[19] M. König, H. Buhmann, L. W. Molenkamp, T. L. Hughes, C.-X. Liu, X.-L. Qi, and S.-C. Zhang, J. Phys. Soc. Jpn **77**, 031007 (2008).
[20] C. Brüne, A. Roth, H. Buhmann, E. M. Hankiewicz, L. W. Molenkamp, J. Maciejko, X.-L. Qi, and S.-C. Zhang, Nature Phys. **8**, 486 (2012).
[21] C. X. Liu, X.-L. Qi, X. Dai, Z. Fang, and S.-C. Zhang, Phys. Rev. Lett. **101**, 146802 (2008).
[22] W. Beugeling, C. X. Liu, E. G. Novik, L. W. Molenkamp, and C. Morais Smith, Phys. Rev. B **85**, 195304 (2012).
[23] R. Yu, W. Zhang, H.-J. Zhang, S.-C. Zhang, X. Dai, and Z. Fang, Science **329**, 61 (2010).
[24] C.-Z. Chang, J. Zhang, X. Feng, J. Shen, Z. Zhang, M. Guo, K. Li, Y. Ou, P. Wei, L.-L. Wang, Z.-Q. Ji, Y. Feng, S. Ji, X. Chen, J. Jia, X. Dai, Z. Fang, S.-C. Zhang, K. He, Y. Wang, L. Lu, X.-C. Ma, and Q.-K. Xue, Science **340**, 167 (2013).
[25] J. G. Checkelsky, R. Yoshimi, A. Tsukazaki, K. S. Takahashi, Y. Kozuka, J. Falson, M. Kawasaki, and Y. Tokura, Nature Phys. **10**, 731 (2014).
[26] A. P. Schnyder, S. Ryu, A. Furusaki, and A. W. W. Ludwig, Phys. Rev. B **78**, 195125 (2008).
[27] C.-K. Chiu, C. Y. Teo, Jeffrey, A. P. Schnyder, and S. Ryu, to be published.
[28] J.-C. Chen, J. Wang, and Q.-F. Sun, Phys. Rev. B **85**, 125401 (2012).
[29] The employed definitions for the QAHL phase and the QSHL phase are physically distinct from the definition used by Chen and co-workers [28].
[30] E. Y. Ma, M. R. Calvo, J. Wang, B. Lian, M. Mühlbauer, C. Brüne, Y.-T. Cui, K. Lai, W. Kundhikanjana, Y. Yang, M. Baenninger, M. König, C. Ames, H. Buhmann, P. Leubner, L. W. Molenkamp, S.-C. Zhang, D. Goldhaber-Gordon, M. A. Kelly, and Z.-X. Shen, Nat. Commun. **6**, 7252 (2015).
[31] L. Du, I. Knez, G. Sullivan, and R.-R. Du, Phys. Rev. Lett. **114**, 096802 (2015).
[32] R. Winkler and U. Zülicke, Anziam J. **57**, 3 (2015).
[33] E. G. Novik, A. Pfeuffer-Jeschke, T. Jungwirth, V. Latussek, C. R. Becker, G. Landwehr, H. Buhmann, and L. W. Molenkamp, Phys. Rev. B **72**, 035321 (2005).
[34] D. Xiao, J. Shi, and Q. Niu, Phys. Rev. Lett. **95**, 137204 (2005).
[35] G. Sundaram and Q. Niu, Phys. Rev. B **59**, 14915 (1999).
[36] P. Streda, J. Phys. C: Solid State Phys. **15**, L717 (1982).
[37] A. Budewitz, K. Bendias, P. Leubner, H. Buhmann, and L. W. Molenkamp, in preparation.
[38] B. Scharf, A. Matos Abiague, and J. Fabian, Phys. Rev. B **86**, 075418 (2012).
[39] G. Tkachov and E. M. Hankiewicz, Phys. Rev. Lett. **104**, 166803 (2010).
[40] U. Rössler, *Landolt-Börnstein: Numerical data and functional relationships in science and technology* (Springer, 1999).
[41] D. G. Rothe, R. W. Reinthaler, C. X. Liu, L. W. Molenkamp, S.-C. Zhang, and E. M. Hankiewicz, New J. Phys. **12**, 065012 (2010).
[42] R. Winkler, *Spin-Orbit Coupling Effects in Two-Dimensional Electron and Hole Systems*, edited by G. Höhler (Springer Tracts in Modern Physics, 2003).
[43] M. Mühlbauer, A. Budewitz, B. Büttner, G. Tkachov, E. M. Hankiewicz, C. Brüne, H. Buhmann, and L. W. Molenkamp, Phys. Rev. Lett. **112**, 146803 (2014).

Appendix A: Parity anomaly and massive topological gauge theory in (2+1)D

In the main text, we discussed how the "parity anomaly" gives rise to a change in Landau level counting in magnetic field and discussed how this fact is related to signatures in the magnetotransport. For this purpose, we compare the continuity equation, derived from the semiclassical equations of motion, with the continuity equation, derived from Maxwell equations, and show that the QAH level has a non-zero Chern number but an effective zero charge carrier density. Therefore, in the process of adiabatically switching on magnetic field, the QAH state can be distinguished from a trivial insulator when the chemical potential is in the mass gap. The structure of this appendix is the following: in the first part, we give an explicit derivation of the "parity anomaly" based

on a semi-classical formulation, while in the second part we show how an additional topological term enters the Maxwell equations. Breaking of parity symmetry due to the Dirac mass term is discussed in Appendix B.

Let us start from the spin-up block of the BHZ Hamiltonian [18], $h_-(\mathbf{k}) = \mathbf{d}(\mathbf{k}) \cdot \boldsymbol{\sigma}$ with $\mathbf{d}(\mathbf{k}) = \left(k_x, -k_y, M^\uparrow\right)$, where we have neglected the k-dependence of the mass term. This approximation is valid in the low energy limit $Ak_f \gg Bk_f^2$ which means at least up to an energy of ≈ 150 meV. Following, we show that the parity-breaking Dirac mass gives rise to an anomalous transverse current response to an applied electric field, as well as to a non-zero carrier density in the ground state. We demand the chemical potential to be located within the mass gap, so that the bulk is insulating and is characterized by a non-zero Chern number

$$\nu^\uparrow = \int^{\mu} \frac{d\mathbf{k}}{2\pi} \Omega_z^\uparrow = -\frac{\operatorname{sgn}\left(M^\uparrow\right)}{2}, \tag{14}$$

where $\mathbf{\Omega}^\uparrow(\mathbf{k}) = \mathrm{i}\nabla_{\mathbf{k}} \times \langle u(\mathbf{k}) | \nabla_{\mathbf{k}} | u(\mathbf{k}) \rangle$ is the Berry curvature and $|u(\mathbf{k})\rangle$ are eigenstates of the Dirac Hamiltonian. In a semi-classical approach the Berry curvature acts as magnetic field in k-space and induces an anomalous correction to the velocity [35]. In order to conserve the phase space volume in magnetic field, it must also enter as a correction in the density of states, whereby the carrier density is given by [34]

$$\begin{aligned} n_e &= \int^{\mu} \frac{d\mathbf{k}}{(2\pi)^2} \left(1 + \frac{e\boldsymbol{H} \cdot \mathbf{\Omega}^\uparrow}{\hbar}\right) + n_{back} \\ &= -\frac{e \operatorname{sgn}\left(M^\uparrow\right)}{2h} H_0, \end{aligned} \tag{15}$$

where n_{back} is a background carrier density and we demand that $n_e(H_0 = 0) = 0$ (bulk insulator). Based on this result, it is straightforward to derive the transverse Hall conductance from Streda's formula [36],

$$\sigma_{xy} = e\frac{\partial n_e}{\partial H_0}\Big|_\mu = -\frac{e^2 \operatorname{sgn}\left(M^\uparrow\right)}{2h}. \tag{16}$$

The result of Eq. (15) and (16) can be combined in a covariant form

$$j_\mu = -\frac{e^2}{4h} \operatorname{sgn}\left(M^\uparrow\right) \epsilon_{\mu\nu\tau} F^{\nu\tau}, \tag{17}$$

where $j^0 \equiv \rho = -en_e$ ($e > 0$) is the charge carrier density and $F^{\nu\tau} \equiv \partial^\nu A^\tau - \partial^\tau A^\nu$ is the electromagnetic tensor. In comparison to the QH effect, where the current originates from the magnetic field and has a $\operatorname{sgn}(eH_0)$-dependence, the anomalous current is hereby induced by the Dirac mass term. Since the mass term breaks parity, this effect in solid state physics is known as "parity anomaly". If the mass term changes sign across a topological domain wall as shown in Fig. 1, charge conservation is violated at the interface, corresponding to a (1+1)D system, known as chiral anomaly,

$$\begin{aligned} \partial^\mu j_\mu &= \frac{e^2}{4h} \left[\partial_x \operatorname{sgn}\left(M^\uparrow(x)\right)\right] \epsilon_{\mu\nu} F^{\mu\nu} && (18) \\ &= \eta \frac{e^2}{2h} \epsilon_{\mu\nu} F^{\mu\nu}, && (19) \end{aligned}$$

where $\eta = \left[\operatorname{sgn}(M^\uparrow(\infty)) - \operatorname{sgn}(M^\uparrow(-\infty))\right]/2$. While the fermion-doubling theorem ensures in even spacetime dimensions that a second domain wall (fermion) must exist which cancels this anomaly in total, there is no such theorem in odd spacetime dimensions [6, 7].

Since the Dirac mass term breaks parity, there is an intrinsic Chern-Simons term (breaks also parity) allowed in the Lagrangian giving rise to topological corrections in the Maxwell equations. The effective Lagrangian of the classical Dirac field is given by $\mathcal{L} = \mathcal{L}_\mathcal{F} + \mathcal{L}_\mathcal{G} + \mathcal{L}_\mathcal{I}$, known as topological massive gauge theory [2, 5]

$$\begin{aligned} \mathcal{L}_\mathcal{F} &= \mathrm{i}\overline{\psi}\partial\!\!\!/\psi - M^\uparrow\overline{\psi}\psi, && (20) \\ \mathcal{L}_\mathcal{G} &= -\frac{1}{4}F^{\mu\nu}F_{\mu\nu} + \frac{\kappa}{4}\epsilon^{\mu\nu\tau}F_{\mu\nu}A_\tau, && (21) \\ \mathcal{L}_\mathcal{I} &= -j^\mu A_\mu \text{ with } j^\mu = -e\overline{\psi}\gamma^\mu\psi, && (22) \end{aligned}$$

where $\mathcal{L}_\mathcal{F}$ describes the fermionic, $\mathcal{L}_\mathcal{G}$ the gauge field and $\mathcal{L}_\mathcal{I}$ the interaction part, $\epsilon^{\mu\nu\tau}F_{\mu\nu}A_\tau$ is the abelian Chern-Simons term and we have used the conventional definitions $\partial\!\!\!/ \equiv \gamma^\mu\partial_\mu$ and $\overline{\psi} \equiv \psi^\dagger\gamma^0$. The gamma matrices fulfill a Clifford algebra $\{\gamma^\mu, \gamma^\nu\} = 2\eta^{\mu\nu}I_4$, where η is the Minkowski metric. While the following derivation is basis independent, we set $\gamma_0 = \sigma_z$, $\gamma_1 = \mathrm{i}\sigma_y$ and $\gamma_2 = \mathrm{i}\sigma_x$ corresponding to the spin-up block of the BHZ Hamiltonian. Using Euler-Lagrange formalism,

$$\partial_\mu \frac{\partial\mathcal{L}}{\partial\left(\partial_\mu A_\nu\right)} - \frac{\partial\mathcal{L}}{\partial A_\nu} = 0 \tag{23}$$

the equations of motion for the gauge field (Maxwell equations) are derived,

$$\begin{aligned} \partial_\mu F^{\mu\nu} + \frac{1}{2}\kappa\epsilon^{\nu\alpha\beta}F_{\alpha\beta} &= j^\nu, && (24) \\ \partial_\mu \tilde{F}^\mu &= 0, && (25) \end{aligned}$$

where the second equation is the Bianchi identity and $\tilde{F}^\mu = \epsilon^{\mu\alpha\beta}F_{\alpha\beta}/2$ is the dual field tensor. For a better visualization, we write out the equation of motions in component form,

$$\begin{aligned} \nabla \cdot \mathbf{E} &= \rho + \kappa H_0 \equiv \rho^\star && (26) \\ \nabla \times \mathbf{E} &= -\frac{\partial}{\partial t} H_0 && (27) \\ \nabla \times \mathbf{B} &= \mathbf{j} + \frac{\partial}{\partial t}\mathbf{E} + \kappa\mathbf{E} \times \mathbf{e}_z, && (28) \end{aligned}$$

where it should be noted that the curl as well as the magnetic field are pseudoscalar in two space dimensions

and $\mathbf{e}_z = (0,0,1)^T$. By deriving the continuity equation from Eq. (26) and (28),

$$\partial^\mu j_\mu = -\frac{1}{2}\partial_x \left[\kappa\left(x\right)\right] \epsilon_{\mu\nu} F^{\mu\nu} \tag{29}$$

and comparing the result with Eq. (17), we find that

$$\kappa = -\frac{e^2}{2h} \mathrm{sgn}\left(M^\uparrow\right). \tag{30}$$

Since $\rho = e^2 H_0 \ \mathrm{sgn}\left(M^\uparrow\right)/2h$ (see Eq. (17)), we find that for an arbitrary magnetic field

$$\nabla \cdot \mathbf{E} = \rho^\star \stackrel{!}{=} 0. \tag{31}$$

This charge is linked to an either filled or empty $n = 0$ LL in the ground state (noting that $n_e = H_0/\phi_0$ corresponds to the carrier density of a single Landau level), where magnetic flux is tied to the electrons.

In an experimental set-up, our theoretical demand of a zero carrier density, $n_e\left(H_0 = 0\right)$, is realized by tuning the carrier density via an external electric gate such that the chemical potential falls into the mass gap. However, we see in the following that instead of the bare charge carrier density ρ, only an effective charge carrier density $\rho^\star$ is accessible by an electric gate.

Finally, we study consequences of a k-dependence of the Dirac mass term as present in Eq. (2) and derive results for the "parity anomaly" accordingly. By using the semi-classical approach, Eq. (15) and (16), we find that the expression for the "parity anomaly" is renormalized by the BHZ parameter B and reads

$$j_\mu = -\frac{e^2}{4h}\left[\mathrm{sgn}\left(M^\uparrow\right) + \mathrm{sgn}\left(B\right)\right]\epsilon_{\mu\nu\tau}F^{\nu\tau}. \tag{32}$$

By including also the quadratic term (Bk^2) in the Lagrangian $\mathcal{L}$ (without writing the calculation explicitly), we find that the Maxwell equations are not changed and our main result, $\rho^\star = 0$, remains valid. The discussion was presented here for the single spin-up block, however it can be analogously repeated for the spin-down block. The experimental signature is determined by the sum of both spin-blocks.

Appendix B: Symmetries of the BHZ Hamiltonian and relation to parity anomaly

The appendix deals with symmetries of the BHZ Hamiltonian, in particular with time-reversal (TRS) and parity symmetry, where the focus is on the latter since we are interested in the origin of the "parity anomaly". Each block of the BHZ Hamiltonian $h_\pm(\mathbf{k})$ (Eq. (2)) can be interpreted as a massive (2+1)D Dirac equation with a k-dependent mass term. At first, we discuss symmetries of a single block and in the second part, we focus on the symmetries of the full BHZ Hamiltonian.

For a single block, invariance under pseudospin TRS (in the band index) implies that an anti-unitary operator $\mathcal{T}$ exists such that [26, 27]

$$\mathcal{T} h_\pm(\mathbf{k}) \mathcal{T}^{-1} = h_\pm(-\mathbf{k}), \tag{33}$$

with $\mathcal{T} = \mathcal{U}\mathcal{K}$ where $\mathcal{U}$ is a unitary matrix and $\mathcal{K}$ is the operator of complex conjugation. Parity symmetry in two space dimensions amounts for e.g. $(x,y) \to (-x,y)$ [8]. Invariance under parity symmetry implies then that a unitary operator $\mathcal{P}_x$ exists such that [32]

$$\mathcal{P}_x h_\pm\left(k_x, k_y\right)\mathcal{P}_x^{-1} = h_\pm\left(-k_x, k_y\right). \tag{34}$$

The mass term (including the Newtonian mass) is odd under both symmetries, e.g. in case of parity symmetry $\mathcal{P}_x = \sigma_2$

$$\begin{aligned} \mathcal{P}_x M_{\mathbf{k}}\sigma_3\mathcal{P}_x^{-1} &= -M_{\mathbf{k}}\sigma_3, \ \ \mathcal{P}_x\epsilon_{\mathbf{k}}\sigma_0\mathcal{P}_x^{-1} = \epsilon_{\mathbf{k}}\sigma_0, \\ \mathcal{P}_x k_x\sigma_1\mathcal{P}_x^{-1} &= -k_x\sigma_1, \ \ \mathcal{P}_x k_y\sigma_2\mathcal{P}_x^{-1} = k_y\sigma_2, \end{aligned} \tag{35}$$

where we have used that $\{\sigma_i, \sigma_j\} = 2\delta_{ij}\sigma_0$. Therefore, pseudospin TRS as well as parity symmetry is broken by the mass term giving rise to the "parity anomaly" in odd spacetime dimensions.

However, in the full BHZ Hamiltonian the anomaly cancels since both spin blocks amount for a different sign in the induced current (compare with Eq. (1)) such that the sum must be zero. The cancellation of the anomalous four-current for the full BHZ model can be also understood in the following way: we can define a TRS as well as parity operator for the full BHZ Hamiltonian connecting both spin blocks $h_\pm$ (similar to a two flavor (2+1)D massive Dirac equation [32]). Such a TRS operator exists and is given by $\mathcal{T}^{BHZ} = -\mathrm{i}\sigma_y \otimes \tau_x K$ while the parity operator is $\mathcal{P}_x^{BHZ} = \sigma_x \otimes \tau_x$. Consequently, there is no "parity anomaly" for the pure BHZ Hamiltonian and the total induced current must vanish.

However, in the presence of an exchange or Zeeman-like Hamiltonian, as given by Eq. (4) and (5), parity as well as TRS are broken, since e.g. $\mathcal{H}_{ex}$ is odd under parity symmetry

$$\mathcal{P}_x^{BHZ}\mathcal{H}_{ex}\left(\mathcal{P}_x^{BHZ}\right)^{-1} = -\mathcal{H}_{ex}. \tag{36}$$

In an external magnetic field (applying Peierls substitution), we find additionally to the Zeeman and exchange interaction that another parity breaking term arises which is given by

$$\mathcal{H}_{Z_D} = \frac{2\pi D H_0}{\phi_0}\mathrm{Diag}\left(1 \ \ -1 \ \ 1 \ \ -1\right), \tag{37}$$

$$\mathcal{P}_x^{BHZ}\mathcal{H}_{Z_D}\left(\mathcal{P}_x^{BHZ}\right)^{-1} = -\mathcal{H}_{Z_D}. \tag{38}$$

All in all, the exchange interaction, the Zeeman as well as the particle-hole asymmetry term break parity and renormalize the effective mass gap in magnetic fields as

highlighted in Eq. (10). A topological transition is therefore driven by an effective g-factor consisting off all three contributions.

Starting from a QSH phase, the total four-current remains zero during an adiabatic increase in the effective g-factor as long as the mass gap of one of the spin-blocks is not closed. If one of the mass gaps is closed, the system enters a QAH (requires ferromagnetic exchange interaction without an external magnetic field) or a QAHL (QAH state in magnetic fields) phase and a non-zero anomalous four-current is observed.

Finally, one should note that a BIA term also violates parity symmetry, where a representation of the BIA term given in the Dirac basis reads [19]

$$\mathcal{H}_{BIA} = -\Delta\sigma_x \otimes \tau_z, \tag{39}$$

$$\mathcal{P}_x^{BHZ}\mathcal{H}_{BIA}\left(\mathcal{P}_x^{BHZ}\right)^{-1} = -\mathcal{H}_{BIA}. \tag{40}$$

where Δ is a parameter. However, Rashba spin-orbit interaction in lowest order [41, 43]

$$\mathcal{H}_R = \begin{pmatrix} 0 & 0 & 0 & \mathrm{i}R_0k_+ \\ 0 & 0 & 0 & 0 \\ 0 & 0 & 0 & 0 \\ -\mathrm{i}R_0k_- & 0 & 0 & 0 \end{pmatrix}, \tag{41}$$

$$\mathcal{P}_x^{BHZ}\mathcal{H}_R\left(kx, ky\right)\left(\mathcal{P}_x^{BHZ}\right)^{-1} = \mathcal{H}_R\left(-k_x, ky\right), \tag{42}$$

where R_0 is a parameter, does not violate parity. Both BIA and Rashba spin-orbit interaction were found to be negligible (less than 1 meV) in recent experiments on symmetric HgTe QWs [43]. Since the mass gap protects the anomalous four-current and, therefore, the "parity anomaly", such small perturbations cannot destroy the "parity anomaly" as long as no gap closing occurs..

Appendix C: Realistic parameters for HgMnTe

This appendix should elucidate how effective BHZ-parameters (see Eq. (2)) for $Hg_{1-y}Mn_yTe/CdTe$ quantum wells have been numerically calculated. These parameters haven been used in the main text to predict an early topological transition in magnetic fields to a $\sigma_{xy} = -e^2/h$ plateau for a 10 nm thick sample of $Hg_{0.98}Mn_{0.02}Te$ as depicted in Fig. 2.

The bulk band structure in case of HgMnTe around the Γ-point is characterized by the 8×8 - Kane Hamiltonian,

$$H\left(\mathbf{k}\right) = H_{Kane} + H_z + H_{ex} + H_s, \tag{43}$$

where H_{Kane} is the bare Kane Hamiltonian, H_z is the Zeeman term, H_{ex} describes sp-d exchange interaction between the s-/p-band electrons and localized d-electrons associated to Mn atoms and H_s amounts for uniaxial strain. The Hamiltonians are discussed in great detail in Ref. [33], where they are written out explicitly in Eq. (6), (14), (20) and (C3), respectively. It is worth noting that Mn does not only give rise to an exchange interaction but one must also renormalize Kane parameters for a given Mn concentration. For small fractions, it is valid to assume that only the band gap parameter $E_g\left(y=0.02\right) \approx -200$ meV is strongly affected [40]. This affects the critical thickness above which HgMnTe becomes a 2D TI , for instance $d_{crit}\left(y=0.02\right) \gtrsim 8.5$ nm, while in pure HgTe the transition should have already emerged at $d_{crit} \gtrsim 6.3$ nm [19].

The full Hamiltonian is then mapped onto a cubic lattice and we assume periodic boundary conditions in x- and y-direction, while in z-direction the interface between HgMnTe and CdTe is taken into account by having z-dependent Kane parameters [18]. Mapping to a cubic lattice corresponds to making use of a finite difference method (also known as tight-binding method), where e.g. a single matrix element with a z-dependent Kane parameter is given by

$$\begin{aligned} k_z\gamma\left(z\right)k_z\left(z\right) &= -\partial_z\gamma\left(z\right)\partial_z\psi\left(z\right) \\ &\approx -\frac{1}{a^2}\left\{\gamma\left(z+\frac{a}{2}\right)\left[\psi\left(z+a\right)-\psi\left(z\right)\right]\right. \\ &\quad \left.-\gamma\left(z-\frac{a}{2}\right)\left[\psi\left(z\right)-\psi\left(z-a\right)\right]\right\}, \end{aligned} \tag{44}$$

where γ is an exemplary Kane parameter, $k_z \to -\mathrm{i}\partial_z$ and in the second step we used a finite difference quotient with grid spacing a. The eigenvalue problem of the Schrödinger equation can then be solved numerically.

Using Löwdin perturbation theory [42] up to the second order, one can derive a low energy model which is valid close to the band gap at the Γ-point. This model is known as BHZ Hamiltonian [18], where

$$H_{BHZ} = \mathcal{H}^{(0)} + \mathcal{H}^{(1)} + \mathcal{H}^{(2)} \tag{45}$$

and

$$\mathcal{H}^{(0)}_{i'i} = \langle i'|H_0|i\rangle, \tag{46}$$

$$\mathcal{H}^{(1)}_{i'i} = \langle i'|V|i\rangle, \tag{47}$$

$$\mathcal{H}^{(2)}_{i'i} = \sum_m \frac{1}{2}V_{i'm}V_{mi}\left(\frac{1}{E_{i'}-E_m}+\frac{1}{E_i-E_m}\right), \tag{48}$$

where $V_{i'm} \equiv \langle i'|V|m\rangle$ and $V_{mi} \equiv \langle m|V|i\rangle$. Moreover, the full Kane Hamiltonian was divided in two parts $H\left(\mathbf{k}\right) = H_0 + V$, where $H_0 = H\left(\mathbf{k}=0\right)$ is the Hamiltonian at the Γ-point and $V = H - H_0$ is treated as a perturbation. The indices $\{i, i'\}$ run over all subbands at Γ forming the basis of the low energy Hamiltonian. In case of the BHZ Hamiltonian this means that $\{i, i'\}$ compose the four subbands $\{|E1,\downarrow\rangle, -|H1,\downarrow\rangle, -|H1,\uparrow\rangle, |E1,\uparrow\rangle\}$. All other subbands are indexed by m and give rise to a renormalization of the bare BHZ parameters. Finally, we end up with the BHZ Hamiltonian as it was explicitly given in Eq. (2). Two exemplary sets of BHZ parameters

for $y = 0.02$ are given in the caption of Fig. 2 of the main text.

Finally, we want to write out the exchange Hamiltonian, $\mathcal{H}_{ex} = \mathrm{Diag}\left(-\chi_E \;\; -\chi_H \;\; \chi_H \;\; \chi_E\right)$, as it was given in Eq. (5), since it is the exchange coupling which dominates in case of HgMnTe the effective g-factor [21, 22]

$$\chi_E = -3\alpha F_1 - \beta F_4 \tag{49}$$

$$\chi_H = -3\beta, \tag{50}$$

where

$$\alpha = -\frac{1}{6} N_1 y S_0 B_{5/2}\left(\frac{5 g_{Mn}\mu_B H_0}{2k_B\left(T+T_0\right)}\right), \tag{51}$$

$$\beta = -\frac{1}{6} N_2 y S_0 B_{5/2}\left(\frac{5 g_{Mn}\mu_B H_0}{2k_B\left(T+T_0\right)}\right), \tag{52}$$

where $S_0 = 5/2$, $B_{5/2}$ is the Brillouin function, $T_0 = 2.6$ K, we assume zero temperature $T = 0$, $N_1 = 400$meV, $N_2 = -600$meV and F_1 and F_4 amounts for S- and P- band character of the $E1$ subband, respectively.

Appendix D: Half-space calculation

In this appendix, we highlight that the property of the $n = 0$ LL being either a solution of the valence band (occupied in ground state) or being a solution of the conduction band (unoccupied in ground state) is already contained in the Landau level spectrum given by Eq. (8). We focus on the spin-up block while the discussion applies analogously to the spin-down block. Therefore, it is possible to make predictions for topological transitions in magnetic field based solely on the expression for Landau level energies. A short prove is outlined in the following based on a half-space calculation [38, 39].

Solutions of the Schrödinger equation on the half space ($y > 0$), $h_-(\mathbf{k} + e/\hbar\mathbf{A})\psi_\uparrow^\eta = E_\uparrow(\eta)\psi_\uparrow^\eta$, are obtained imposing the ansatz $\psi_\uparrow^\eta(\tilde{y}) = \left(\begin{array}{cc}\tilde{u}_1 D_{\eta-1}(\tilde{y}) & \tilde{u}_2 D_\eta(\tilde{y})\end{array}\right)^T$, where $\tilde{y} = \sqrt{2}\left(y - y_k\right)/l_H$, $y_k = l_H^2 k_x$ and D_η are parabolic cylindrical functions. The eigenvalue problem is solved using the recurrence relations

$$\left(\frac{\tilde{y}}{2} \pm \partial_{\tilde{y}}\right) D_\eta(\tilde{y}) = \begin{cases}\eta D_{\eta-1}(\tilde{y}) \\ D_{\eta+1}(\tilde{y})\end{cases}, \tag{53}$$

$$\left(\frac{\tilde{y}^2}{2} - \partial_{\tilde{y}}^2\right) D_\eta(\tilde{y}) = \left(\eta + \frac{1}{2}\right) D_\eta(\tilde{y}). \tag{54}$$

After a straightforward calculation, it follows that the spectrum is again given by Eq. (8),

$$E^{\pm}_{\uparrow,\eta>0} = \frac{g_1 - \beta}{2} - \eta\delta \pm \sqrt{\eta\alpha^2 + \left(M_\uparrow^\star(H_0) - \eta\beta\right)^2}, \tag{55}$$

where $\alpha = \sqrt{2}A/l_H$, $\beta = 2B/l_H^2$ and $\delta = 2D/l_H^2$, $g_{1/2} = (\chi_E + g_E H_0) \pm (\chi_H + g_H H_0)$, $M_\uparrow^\star(H_0) = M + g^\star(H_0)$ with $g^\star(H_0) = \left(g_2(H_0) - \delta(H_0)\right)/2$ as in the main text. However, with the difference that $n \in \mathbb{N}$ is replaced by $\eta \in \mathbb{Z}$. Obviously, there are in general two solutions with $\eta = 0$, where the respective "$-/+$" - sign in Eq. (55) symbolizes that the $n = 0$ LL belongs either to the valence or to the conduction band. This is in contrast to the pure bulk calculation presented in the main text, where the eigenvalue of the $n = 0$ LL is comprised within a single expression (see Eq. (9)). This is due to the fact that the boundary conditions have already been applied in the bulk calculation by choosing the Hermite polynomials as solutions.

A solution of the eigenvalue problem is given by

$$\Psi(\tilde{y}) = c_1\psi_{\eta_1}(\tilde{y}) + c_2\psi_{\eta_2}(\tilde{y}) + c_3\psi_{\eta_1}(-\tilde{y}) + c_4\psi_{\eta_2}(-\tilde{y}), \tag{56}$$

where we have used that $D_\eta(\tilde{y})$ and $D_\eta(-\tilde{y})$ are two independent solutions,

$$\eta_{1/2} = \frac{1}{2\left(\beta^2 - \delta^2\right)}\Big[-\alpha^2 + 2\beta M_\uparrow^\star + 2\delta\epsilon \pm \sqrt{\alpha^4 - 4\alpha^2\left(\beta M_\uparrow^\star + \delta\epsilon\right) + 4\left(\beta\epsilon + \delta M_\uparrow^\star\right)^2}\Big] \tag{57}$$

and $\epsilon = E + (\beta - g_1)/2$. By applying the boundary conditions, $\psi(y = 0) = 0$ and $\lim_{y\to\infty}\psi(y) = 0$, we find that only one $\eta = 0$ solution is allowed. Depending on whether $M_\uparrow^\star/B > 0$ or $M_\uparrow^\star/B < 0$, the $n = 0$ LL belongs either to the valence or to the conduction band, respectively. Such a topological transition in magnetic field is shown in Fig. 4. Here, the $n = 0$ LL changes from the valence (Fig. 4 a)) to the conduction band (Fig. 4 b)) and the transition point is marked by a massless Dirac fermion, $M_\uparrow^\star = 0$ as we accordingly found in Appendix A. While the discussion here was only given for the spin-up block, a transition can occur either for the spin up or the spin-down block depending on the sign of the effective g-factor as discussed in the main text.

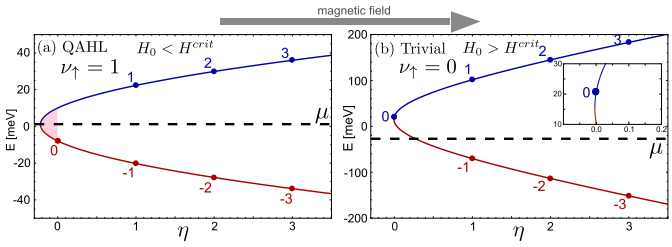

FIG. 4. In **(a)** and **(b)** solutions $E_\uparrow(\eta)$ in the bulk limit $y_k = l_H^2 k_x \gg 0$ are indicated by points (toy parameters). In this limit, η converges against integer-values. Along the topological transition (for $\mathrm{sgn}(eH_0) > 0$ and $\mathrm{sgn}(g^\star) > 0$), the $n = 0$ LL changes from (a) the hole (red) to (b) the particle branch (blue). To highlight the branch change, the inset in (b) shows enlarged the $n = 0$ LL. The chemical potential at constant effective carrier density $\rho^\star$ is indicated by the dashed line. During the transition the Chern number changes from $\nu_\uparrow = 1$ to $\nu_\uparrow = 0$.